Side Forces on Unyawed Slender Inclined Aerodynamic Bodies

Hsiao C. Kao*
Northrop Corporation, Hawthorne, Calif.

Wind tunnel tests in recent years have indicated the existence of nonzero side forces and yawing moments on a fuselage model, configuration build-up, and a complete airplane model at high angles of attack but zero angle of sideslip. These forces and moments are a potential hazard to aircraft stability and control. Based on observations in some related experiments, theoretical consideration and finally some interpretation of our own, a simple model is proposed to describe the flow characteristics of these nonzero forces and moments. A prediction method resulting from this model with correlation parameters taken directly from the published papers is formulated. The calculated results are compared with low-speed test data of a 10% scale F-5E fuselage model and a circular tangent ogive with afterbody and show satisfactory agreement.

Nomenclature

A = model wing area, 1.86 ft^2
B_c = empirical constant for prediction of critical angle of attack
b = model wing span, 2.67 ft
C_m = circulation around body between g_{m-1} and g_m
C_n = yawing moment coefficient, moment/$\frac{1}{2}\rho_\infty U_\infty{}^2 Ab$
C_y = side force coefficient, force/$\frac{1}{2}\rho_\infty U_\infty{}^2 A$
d = diameter or mean diameter of afterbody
g_m = distance of vortex line m along body axis
g' = interval between two consecutive vortex lines
L = lift or lateral force per unit length
R_c = cross-flow Reynolds number, $U_\infty d \sin\alpha/\upsilon$
R_D = Reynolds number based on diameter, $U_\infty d/\upsilon$
S = Strouhal number
U_∞ = freestream velocity
α = angle of attack
α_c = critical angle of attack corresponding to onset of flow asymmetry
α_m = angle of attack for a local peak m of nonzero side force
Γ = vortex strength
Θ_c = semi-apex angle
υ = kinematic viscosity
ρ_∞ = freestream density

Introduction

IN spite of the fact that flow separation has haunted engineers for so long a time, the recent discovery of nonzero side forces experienced by various bodies, ranging from a fuselage model through configuration build-up to a complete airplane model, reveals an additional adversity. Nonzero side forces and hence yawing moments are defined here to be side forces and yawing moments on a slender body at an angle of attack but zero angle of sideslip. These side forces and yawing moments, whose magnitude may become as large as or even larger than the normal force at sufficiently high angle of attack, are a potential hazard to the stability and control of modern fighter aircraft and missiles.

The existence of nonzero forces has been known for a fairly long time[1,2] but has received little attention until some recent investigations. The scope of these investigations has, however, been largely limited to wind tunnel tests and correlations of pertinent parameters (see, for example, Refs. 3-5), with two known exceptions that Lamont and Hunt[6] and Wardlaw[7] present semiempirical prediction methods in addition to test data. Unfortunately, it is also apparent that experimental results by different investigators are not always in agreement. One of the reasons, apart from experimental inaccuracy, may be that a small variation of one of many parameters causes substantial deviation. This fact has been amply illustrated by Keener and Chapman.[5]

A rather surprising finding from Franco's test data[3] at Northrop is that such a nonzero side force and moment occurred not only on fuselages but also on a 10% scale F-5E complete airplane model (Figs. 1 and 2). A possible explanation is that the geometry of the forebody being a dominant factor in producing nonzero side forces (as also pointed out by Keener and Chapman) overwhelms the effect from wing and tails. Thus, addition of these elements merely changed its magnitude and "frequency" but did not hinder its occurrence. (The word frequency is used loosely here to indicate the status of repeated occurrence of the peaks and valleys of the nonzero side force and yawing moment).

After Franco's test data became known, an analysis was subsequently made to identify the source of these nonzero side forces, from which the present semiempirical approach resulted. This method in the present form applies only to fuselage or slender inclined bodies; it is, however, hoped that a modified version will be developed for application to a fuselage with interference surfaces, such as wing and tails, and with the influence of Mach number included. The predictions made so far have been found to agree with most of the salient features observed in Franco's experiment. These calculations were made independently and prior to the publication of Lamont and Hunt's work. Thus, even though both methods are based on the cross-flow analogy, the details are radically different. However, an additional reason to prompt writing of this note is that Franco's test indicated unmistakenly the periodic nature of these nonzero side forces against angle of attack with alternate sense, whereas Lamont and Hunt's experiment revealed only wavelet oscillations on a dominant hump. The Reynolds numbers in these experiments may have been somewhat different, but the bodies were of comparable fineness ratios.† Modelled from the test data, our calculations, therefore, show periodicity and theirs does not. To resolve these questions, it is evident that further studies are

Received October 5, 1973; revision received October 2, 1974. The author wishes to express his appreciation to P. T. Wooler, and S. A. Powers of Northrop Corp. for calling attention to this problem.

Index categories: Aircraft Aerodynamics (Including Component Aerodynamics); Aircraft Performance.

*Senior Scientist, Aerodynamics Research, Aircraft Division.

†The Reynolds number in Franco's experiment based on the mean diameter of the fuselage model was approximately 0.6×10^6; the cross-flow Reynolds number at a typical incidence of 35° was then about 0.3×10.[6]

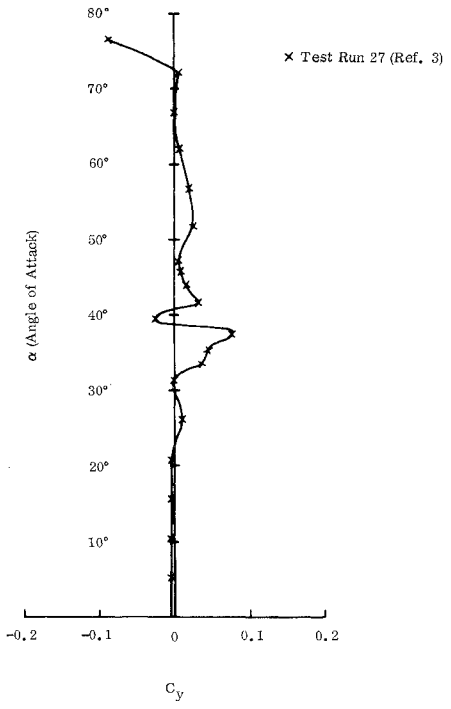

Fig. 1 Side force coefficient on 0.1 scale F-5E complete configuration model (fuselage, wing, vertical and horizontal tails) at zero sideslip angle.

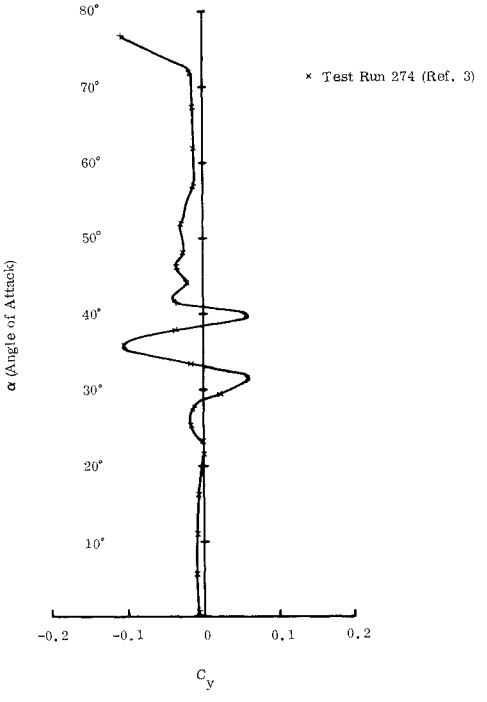

Fig. 2 Side force coefficient on 0.1 scale F-5E complete configuration model with center-line 275 gal tank (fuselage, wing, vertical and horizontal tails, and external tank) at zero sideslip angle.

required and the purpose of this paper is to stimulate this undertaking in addition to presentation of our method.

During the period of revision, Wardlaw's[7] and Keener and Chapman's[5] work became known. The former introduces a different and more theoretical-oriented approach for prediction, but the test data seem to show fewer local peaks (a valley is a negative peak) than those in either Franco's test or Keener and Chapman's experiment of a tangent ogive with an attached afterbody. And the latter is mainly a study of forebodies. Only limited data were presented with afterbodies attached. Because of the slenderness requirement in the present method, only these data with afterbodies were used to compare with calculated values.

Prediction Method

The proposed model is based partly on theoretical considerations and partly on experimental observations. The parameters required in the calculation are nearly all taken from the published papers in the related experiments. The first part of this section is devoted to justification or theoretical consideration and the second part to basic formulas.

Justification of the Proposed Model

The concept of cross-flow analogy or the slender body theory has been well known and widely used since Munk's paper of 1924. It was originally based on the observed fact that "the air gives way to the passing slender body by flowing around the axis of the body, not by flowing along it," and applied to the inviscid flow calculations. However, as the angle of attack increases, the prediction of lift coefficient on a slender body with abrupt base becomes increasingly worse by considering the inviscid force alone. Consequently, a modification was made by Allen and Perkins[1] to include the viscous separation effect which greatly improved the calculated results. In the same vein, we adapt this idea to the flow with separation inducing not only the normal force as already accounted for by them but also the lateral force.

Based on this idea of similitude (called the impulsive flow analogy in Ref. 8) the flow over the inclined body viewed in the cross-flow plane is time-dependent and has a trailing vortex wake, which grows with time much like the growth and shedding of vortices behind a two-dimensional body impulsively started from rest with a velocity equal to the cross-flow velocity of $U_\infty \sin\alpha$. (U_∞ is the freestream velocity and α the angle of attack). A very illuminative depiction of the trailing vortices and the cross-flow plane can be found in the work of Thomson and Morrison[8] and is reproduced here as Fig. 3. The lateral force on the inclined body again viewed in the cross-flow plane is then equivalent to the lift. As is well known, a nonzero circulation around a cylinder sustains a lift. This lift is furthermore independent of the form of the cylinder by the theorem of Kutta and Joukowski. Therefore, if we associate the lateral force with the lift and find a way to estimate the circulation, the nonzero side force on an inclined body of arbitrary shape will be known. For this reason, the occurrence and prediction of the circulation are the main consideration in proposing the present model and prediction method.

One complication, which has not been mentioned so far, is that there now exist singularities (point vortices) in the flowfield in addition to the circulation. The singularities will also exert forces on the cylinder, much like the trailing vortex sheet making contribution to the lift on an oscillating airfoil. These forces are, however, considered to be small in the present model and are assumed to be negligible compared to the lift due to circulation. After a better description of the vortex wake is given, we will return to this point.

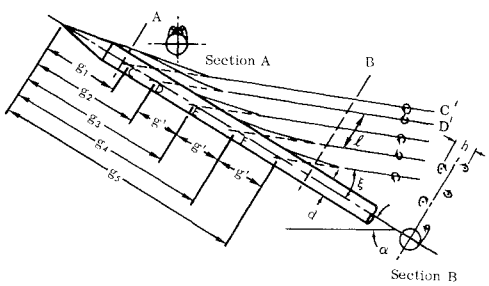

Fig. 3 A sketch of vortex wake over a slender cylindrical body from Thomson and Morrison.

When a cylinder is started impulsively from rest, the flow is initially in a state of potential flow but quickly forms a boundary layer which, in turn, separates and develops into a pair of symmetric "point" vortices. This pair of symmetric vortices is, however, not stable. As time elapses, one of them will be washed away and the flow becomes asymmetric. In Ref. 9 after observation of a motion picture, Sarpkaya concluded: "The symmetrical vortices that form at the start of motion oscillate back and forth, mainly in the direction of the ambient flow, and grow or diminish in intensity prior to the actual shedding of the first vortex." This observation is further supported by the findings of Thomson and Morrison,[8] in which the measured strength of two outmost vortices are found to be unequal. Sarpkaya's observation explains not only the onset of circulation, for which some detailed argument will be given, but also the occurrence of a number of small, oscillatory side forces at moderate angle of attack.

Before the nose of a slender body first penetrates the cross-flow plane, the flow is irrotational and will remain so at subsequent time provided that the closed material line to be followed is sufficiently large. However, as soon as the initial pair of vortices oscillates, grows and diminishes in intensity, an imbalance of the combined vortex strength results. This imbalance will then be compensated for by a circulation about the cylinder in accordance with the theorem of constancy of circulation. Accordingly, the lateral force is expected to occur at the same time as transition of the symmetric vortices takes place. For example, the small oscillatory side forces prior to the major peak at $\alpha = 36.5°$ (in Fig. 4) are believed to be attributed to this.

With the appearance of circulation in the flow, the velocity around the cylinder is asymmetric, being faster on one side and slower on the opposite. This will further result in promoting and sustaining the process of alternate vortex shedding. However, as the third and subsequent vortices are being cast off, alternating vorticity is continually added to the fluid. To maintain the constancy of circulation along a material line large enough to encircle all vortices and the cylinder, the intensity of circulation around the body will have to alter. Since the vorticity is continually being created in the boundary layer and cast off through the "feeding sheet" to form a new vortex, it is an endless attempt to achieve a balance in the system that, in turn, results in endless cycles of alternate circulations around the body. To confirm this argument, we refer to the experiment made by Drescher and depicted in Fig. 5. Although only the force is indicated in these diagrams, the existence of circulation can be deduced from the occurrence of lift. In addition, Plate 24 in Prandtl and Tiejens' monograph[10] would also suggest this sequence of events.

The circulation around the cylinder in the present model coexists with a system of singulatrities (point vortices); these singularities also give rise to forces on the cylinder in accordance with Lagally's theorem (see, for example, Milne-Thomson[11] for more details). The total force is, however, the sum of additive forces induced by individual singularities, whose magnitude is proportional to the square of singularity strength but diminishes with the distance from the cylinder at a rate much faster than the first power. These forces can, in principle, be included in the prediction method. (For a cross section other than a circular cylinder, conformal mapping will have to be employed). However, due to the approximate nature of the method and the assumption that the circulation is sufficiently large and no strong vortex is located near the cylinder, we neglect these forces due to singularities and assume the side force being simple equal to the lift induced by circulation alone. It follows that in the cross-flow plane the usual formula for lift applies

$$L = \rho_\infty U_\infty \Gamma \sin\alpha \tag{1}$$

The symbol L denotes the lift or the lateral force per unit length of the cylinder, ρ_∞ is the density, Γ the circulation, and

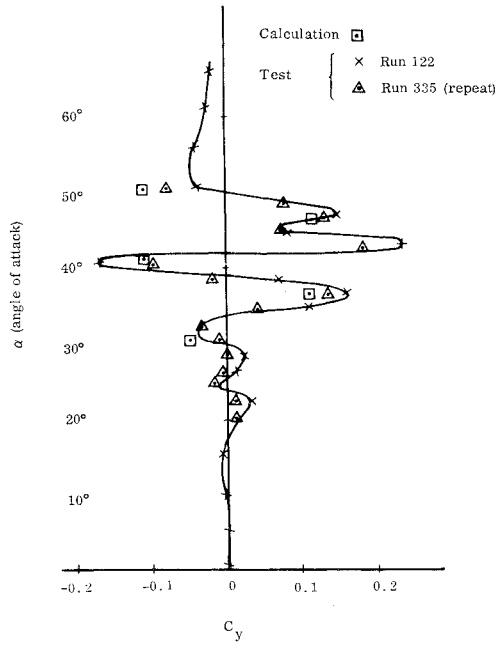

Fig. 4 Side force coefficient on 0.1 scale F-5E fuselage model at zero sideslip angle.

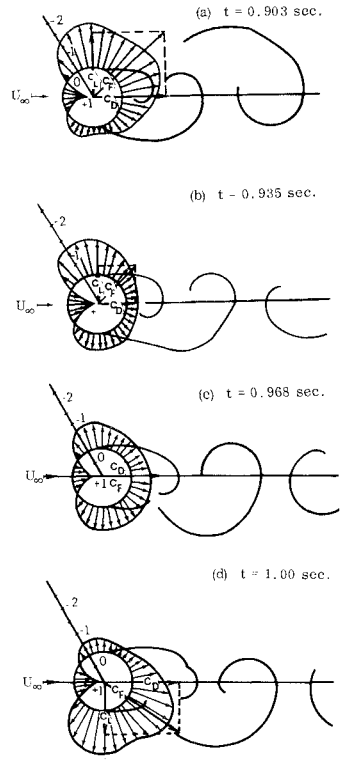

Fig. 5 A sequence of simultaneous pressure fields and wake forms at $R_D = 1.13 \times 10^5$ from Drescher (Figure taken from Ref. 14).

$U_\infty \sin\alpha$ the freestream velocity in the cross-flow plane.

As noted previously, this force is independent of the body shape. Consequently, if we have a method to estimate the circulation, this formula will then give the side force per unit length from which the yawing moment is known. It is, however, not possible at present to give an estimate of this circulation by theoretical consideration alone, since the formation of the vortex wake behind a bluff body involves not only the boundary-layer separation but also other complex processes, and recourse to a semiempirical method is essential. One such method, that we propose to follow here, is to

make prediction and give estimate of the sense and intensity of free vortices on the basis of the existing experimental findings. Using this as an input and by means of the theorem of constancy of circulation, we obtain the circulation.

The task now reduces to the treatment of the free vortices. To formulate the problem, we have to describe these vortices in terms of fluid mechanical properties. Some of these are: the incipient condition for vortex shedding, the time interval between each vortex breakaway, the relationship between the body length and vortex shedding, and the spacing and strength of these free vortices. Fortunately, most of these questions have been investigated by Thomson and Morrison[8] in an elaborate experiment. These experimental findings in conjunction with others as quoted in Refs. 9, 13, and 14 can be moulded to form an empirical but quantitative representation of this free-vortex system. A step-by-step procedure of how this is to be done will be presented.

Prior to this, a word or two seems in order to qualify the aforesaid Lagally's theorem. The usual presentation of this theorem is valid for a stationary system. If the free vortices in a uniform stream change their position and strength with time, modification will have to be made. For this we refer to the work‡ by Sarpkaya.[12] These unsteady variations are, however, to be neglected here under the assumption that the rate of the change of the vortex intensity is not important and the relative velocity of the free vortices to the body is small compared with the cross-flow freestream velocity.

Basic Equations

The most important inputs required in the present model are the quantitative representations of the number and the total intensity of free vortices in the wake of every cross-flow plane. The information for the number of free vortices, which is clearly related to the mechanism of vortex detachment, may be eventually related to the so-called "frequency," i.e., the condition of repeated occurrence of local peaks and valleys of nonzero side forces. The total intensity is associated directly to the strength of circulation, which, in turn, gives the magnitude of the side force. To this end, we have two equations for these two quantities. Once the frequency and magnitude become known, the representation of the nonzero side force and also the yawing moment is virtually complete.

The form of these two equations has actually been given by Thomson and Morrison as a part of their theoretical considerations under the concept of cross-flow analogy (or called the impulse flow analogy by the authors). But these are merely two relationships for different flow quantities. To use them as working equations, we have to reduce the unknowns to one for each equation. One method to meet this requirement is that we introduce more empirical correlations. In this connection, we refer to the work by Thomson and Morrison,[8] Peake, Rainbird, and Atraghji[13] and Morkovin.[14]

The dispositon of the vortex wake over a fuselage is assumed to be similar to those observed in Ref. 8 over cylindrical bodies. On the basis of this idealization, the spacing, position and breakaway points of vortices can be estimated in a similar manner.

To do this and from the definition of the Strouhal number S in the cross-flow plane, we have

$$S = nd/U_\infty \sin\alpha$$

where the symbol d refers to the diameter of the cylinder and n to the shedding frequency of like-sign vortices, from whose definition it follows that the time interval between vortices of like sign is simply $1/n$. In reference to Fig. 3, this is also the time for a fluid particle to traverse a distance $2g'/U_\infty \cos\alpha$ with the freestream velocity equal to U_∞. Upon substitution of this quantity, the previous equation takes the form

$$g'/d = 0.5/(S \tan\alpha)$$

If the cross-flow analogy were exact, the vortex wake were completely stable, the spacing between vortex lines were uniform, no Mach number and Reynolds number effects were present, etc., the mean dimensionless quantity $g'S \tan\alpha/d$ measured in wind tunnel test would be equal to 0.5. Instead, this value is chosen to equal 0.35 here, which agrees with the lower limit indicated in Ref. 8. We thus modify the definition to the form

$$g'/d = 0.35/(S \tan\alpha) \qquad (2)$$

This is then our first working equation for determining the interval between vortex lines with the body diameter, incidence and the Strouhal number given.

The question of what value to choose for the Strouhal number is still open. The following reasoning, however, indicates that it is a constant under the intended conditions of the present model. The cross-flow Reynolds number, which is defined as $R_c = U_\infty d \sin\alpha/\nu$, with ν being the kinematic viscosity, is estimated to be around 3×10^5 in our low speed wind tunnel using the 0.1 scale F-5E model and with angles of attack varying from 10° to 50.° The Strouhal number, corresponding to this range of Reynolds number, for a two-dimensional circular cylinder is known to be approximately equal to 0.2 (see Fig. 6 for Morkovin's compilation[14] of numerous test results). To make certain that this value is also applicable to inclined bodies and also to study the Mach number effect, Thomson and Morrison conducted a series of experiments within their attainable Reynolds number range and concluded that 0.2 is indeed an accurate representation of Strouhal number for an inclined body at low speed. Hence, in place of S in Eq. (2) we will use 0.2 for computation, including the example of a tangent ogive with afterbody in Fig. 7. The cross-flow Reynolds number for this latter case was estimated to be under $5\times10.^5$ Thus far we have essentially completed the discussion for the first working equation, save some statements for qualifying the arguments so as to further clarify the matter.

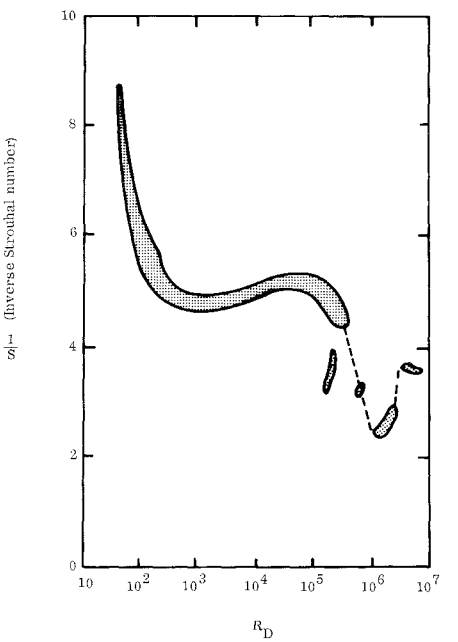

Fig. 6 Strouhal number of circular cylinders across Reynolds number range based on diameters from Morkovin.

‡The equation for the lift in this paper is incomplete in the sense that the most important effect, the circulation around the cylinder, is not accounted for. For a general distribution of vortices, which it implies, the net intensity of all free vortices is not necessarily zero and the circulation about the cylinder should not be omitted.

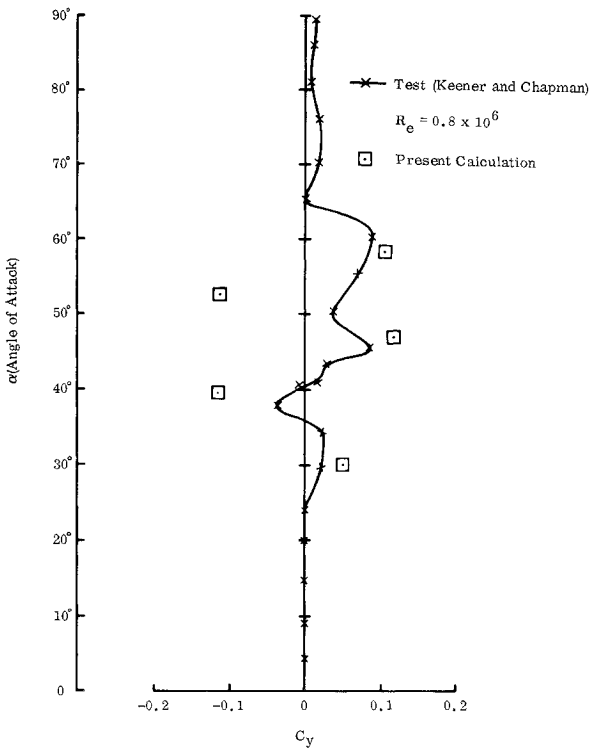

Fig. 7 Side force coefficient in circular tangent ogive with attached afterbody at zero sideslip angle.

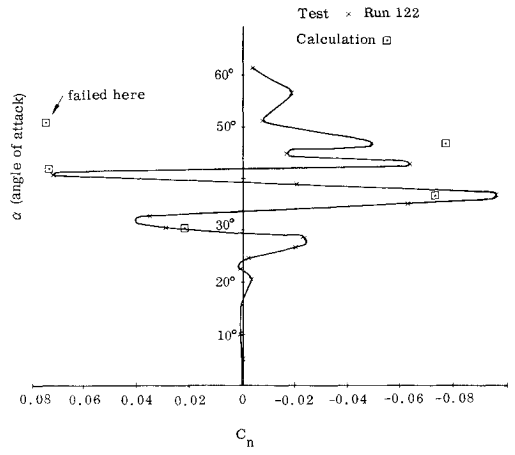

Fig. 8 Yawing moment coefficient on 0.1 scale F-5E fuselage model about body axis and at zero sideslip angle.

For one thing, the correlation formulas, on which we base the present prediction method, are mostly obtained from experiments using cone-cylinder or ogive-cylinder combinations. The main configuration to be concerned here is, however, a fuselage, which usually has an ogive-like forebody but whose afterbody is generally quite different from a circular cylinder. The assumption made here is that the forebody and the fineness ratio are the dominant factors to the disposition of the vortex wake but not the detailed geometry of the afterbody. To this end, the diameter d in Eq. (2) may be chosen as an average diameter of a fuselage. This point will be further discussed after the second working equation is presented.

As mentioned previously, Eq. (2) will be eventually used to determine the angles of attack corresponding to the local peaks and valleys of nonzero side forces. Since it is not obvious how this can be done, it is perhaps worth stating the underlying elements at this juncture and leaving the details to the next section. To connect the disposition of vortex lines measured by g' in the present formulation to the angles of attack for local peaks (a valley is a negative peak), we have to invoke the following idealization. Notice here that we have drawn straight lines to approximate the actual vortex lines in Fig. 3. When one of these simplified vortex lines comes in contact with the base of the fuselage, we assume that the lateral force exhibits a local maximum or minimum. This, therefore, implies that the present prediction method is only capable to disclose informations about the local peaks as shown by open square symbols in Figs. 4 and 8. For practical purposes these values are perhaps the most important quantities to characterize the nonzero side forces.

This idealization may sound arbitrary at first glance, but it is possible to find some evidence from Drescher's experiment to show its validity. A close inspection of four pictures in time sequence given in Fig. 5 will lead to the conclusion that the lift is maximum when the vortex around the cylinder reaches its maturity and begins to detach.

Equation (2) is derived on the basis of the so-called regular vortex disposition, i.e., the first pair has been excluded. Since these two vortices are initially formed at the ogive-like nose region and detached by a different mechanism as stated earlier, it is natural to make a separate estimate. For the detail, we again defer it to the next section. Here we only remark parenthetically that the interval g' in Fig. 3 begins at point D; the distance between C and D is not marked but is not g.'

Returning now to the second working equation, once more we idealize the complex situation by making an assumption that as far as the intensity is concerned, the regular vortices viewed in the cross-flow plane are similar to the Karman vortex street of infinite extent.§ Using the cross-flow analogy leads immediately to the formula[8,11]

$$\frac{\Gamma}{U_\infty d \sin\alpha} = \frac{2X(1-X)}{S} \coth \frac{\pi h}{\mathfrak{L}} \qquad (3)$$

where Γ is the strength of a detached vortex, h the lateral spacing between the vortex rows, and $\mathfrak{L}$ the normal spacing between vortices of like sign. The symbol X is defined as $X = \tan\xi/\tan\alpha$, with ξ being the inclination angle of a vortex line (Fig. 3). The quantity $h/\mathfrak{L}$ is the ratio of the transverse to the longitudinal spacing; its average value is known to be approximately a constant and equal to 0.19 by estimating from schlieren photographs (Ref. 8).

Application of Eq. (3) requires determination of X. Fortunately, it was again found in Ref. 8 to be approximately a constant. We choose $X = 0.8$ for the present purpose in compliance with the line of best fit.

Thomson and Morrison[8] stated that Eq. (3) over-predicted the vortex strength. This over-prediction is actually considerable; the ratio of the vortex strength $\Gamma/U_\infty d \sin\alpha$ computed from Eq. (3) to the mean value of measurements made by these authors is approximately 3:2 in the low-speed and low Reynolds number range covered ($R_c \approx 10^5$). We, however, use this equation directly without modification in calculation of the nonzero side force and yawing moment on the F-5E fuselage model. This implies in effect that a geometric factor has been included to account for the irregular shape of the afterbody, for it is conceivable that the

§The wake behind a cylinder in a two-dimensional flow is known to exhibit some form of periodicity in a fairly wide range of Reynolds numbers. However, the periodic wake referred to the Karman vortex street, which is mostly laminar and has a stable configuration with the ratio of the transverse to the logitudinal spacing equal to approximately 0.28, makes its appearance generally in the Reynolds number below 150-300 based on the body diameter. Although the cross-flow Reynolds number in Thomson and Morrison's experiment was around 7.5×10^4, the wake in the schlieren pictures appears to resemble the Karman vortex street and the intensity of a vortex may be estimated by Eq. (1)-(3). The ratio $h/\mathfrak{L}$ was, however, found to be different from 0.28 and fixed approximately to be 0.19 after analyzing the data.

intensity is reinforced by lack of regularity. The agreement between the prediction and test as shown in Fig. 4 and 8 seems to attest this argument.

For the side force predication on the cylindrical afterbody, such as the one indicated in Fig. 7, we will reduce the intensity calculated from Eq. (3) by a factor of 2/3. This additional empiricism could have actually been avoided, provided that we make use of the so-called sweepback principle (Ref. 8) rather than the cross-flow analogy. The reason that the latter is retained is simply because we place more emphasis on the fuselage prediction.

With the vortex intensity now specified, application of Kelvin's circulation theorem gives the circulation around the fuselage which, in turn yields the lift (side forec) per unit length by means of Eq. (1).

Calculation Procedure

In this section, we will present mainly the procedures of appying Eqs. (2) and (3) to result in numerical values.

Prediction of Angle of Attack for a Local Peak

To begin with, we must deal with a more difficult problem of how the first pair of vortices detach themselves, their controlling parameters, and the critical angle of attack for the incipience of asymmetric forces. To answer these questions, we have recourse to experimental results. Here we quote only the relevant work by Peake, Rainbird, and Atraghji[13] and Keener and Chapman.[5]

Equation (2) as it stands is merely a relationship of the interval between vortex lines, the incidence, and the Strouhal number. By means of the idealization stated earlier that when one of the simplified vortex lines reaches the fuselage base the side force exhibits a local peak, we associate this equation with the local peak but we still cannot obtain a numerical value, because the initial distance g_2 (Fig. 3) is not known. This information cannot be acquired theoretically at present, since the mechanism for detachment of the initial pair is too complex to be handled properly.

Although the onset of flow asymmetry is probably influenced by many parameters, the more important ones seem to have been investigated. For instance, Fig. 9 is a graphical representation of these parameters. (A similar depiction is also included in Ref. 5). In reference to this figure, we notice that for a given Mach number and Reynolds number the semiapex angle Θ_c appears to play a dominant role. The fineness ratio also shows its effect but to a less extent. To

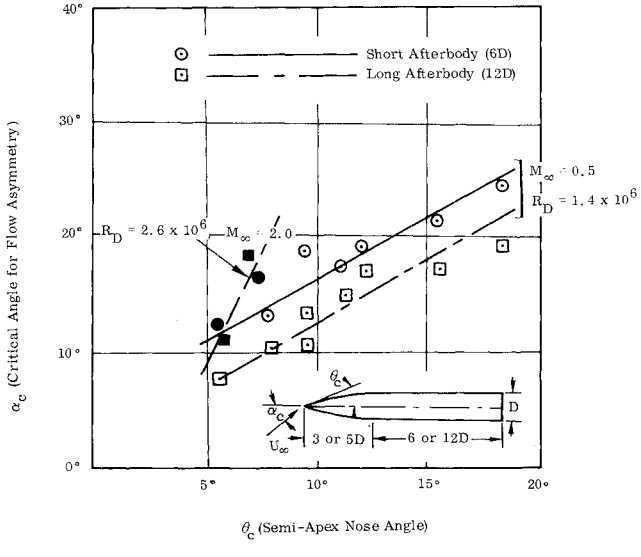

Fig. 9 Critical angle of attack for onset of flow asymmetry about slender cylindrical bodies from Peake, Rainbird, and Atraghji.

make the estimate, we assume that the form of Eq. (2) is also applicable to the detachment of the initial pair, provided that a new empirical constant, which was fixed to be 0.35 earlier, can be properly selected.

In the process of increasing angle of attack, we will first encounter a situation where the vortex wake over the body base viewed in the cross-flow plane consists of two vortices, one of which has been washed away and the remaining one is on the verge of detachment. In other words, the distance g_2 is equal to the body length. We construe this to indicate the incipience of asymmetric force.

For the simple configuration, such as the tangent ogive with afterbody in Fig. 7, which has a semiapex angle of 16.5° and the fineness ratio equal to 7, the critical angle-of-attack α_c for the onset of flow asymmetry has been determined and is estimated to be 30° from Ref. 5. Invoking the aforesaid idealizations, we obtain the empirical const B_c from Eq. (2) as follows:

$$B_c = (g_2/\mathrm{d})S \tan \alpha_c = 0.809$$

where the Strouhal number has been taken to be 0.2 for the reason previously noted. The angle-of-attack α_3 for the next local peak for which $g_3/\mathrm{d} = (g_2 + g')/d = 7$ is given by

$$\tan \alpha_3 = (B_c + 0.35) \div \frac{(g_2 + g')S}{\mathrm{d}} = 0.827$$

Similarly, $\alpha_4 \ldots \alpha_m$ can be evaluated. To write symbolically, we have

$$\tan \alpha_m = \frac{B_c + 0.35(m-2)}{f_r S} \quad \text{for } m \geq 3, \tag{4}$$

where f_r refers to the fineness ratio. The angles so computed for this case are shown in Fig. 7.

Since the experimental data for the critical angle of attack are not always available especially for the more complicated configurations such as a fuselage, to claim this to be a prediction method we must find a way to evaluate B_c from test data of related experiments conducted for bodies other than the one to be examined. To illustrate how this is done, we use the F-5E fuselage model as a working example and make a cross-reference to test data on a cone-cylinder combination. The critical angle-of-attack α_c for this body with the fineness ratio of 9 (their short afterbody) and the semi-apex angle of 15° is found from Fig. 9 to be approximately 22.5°. It follows by means of the aforesaid idelaization that g_2/d is equal to the fineness ratio 9 and Eq. (2) reduces to

$$B_c = (g_2/d)S \tan \alpha_c = (9 \tan 22.5^\circ)D \tag{5}$$

The Strouhal number in this equation is, however, not equal to 0.2, because the Reynolds number based on the diameter in their experiment was $1.4 \times 10,^6$ which is believed to be in the transition region instead of the laminar flow in the previous case. The Strouhal number in the transition region is much different from that of laminar flow (Fig. 6), and the value of S in Eq. (5) is estimated to be 0.35. With this specified, B_c is found to be 1.3. The F-5E fuselage model has an ogive-like forebody with the mean semiapex angle Θ_c of 15.° The overall length is 4.5 ft and the mean base diameter is about 0.4 ft; the fineness ratio is then approximately 11.2. Since the semi-apex angles of these two bodies are the same and the finess ratios are comparable, we assume that the empirical constant B_c obtained for the first body stays unchanged for the second. The test for the fuselage was, however, conducted in the laminar region; the critical angle-of-attack α_c would necessarily be different from 22.5.° To estimate this, we again

make use of Eq. (2), which leads to

$$\tan \alpha_c = B_c/(g_2 S/d) = 0.58 \qquad (6)$$

The angles of attack for other local peaks $\alpha_3 \ldots \alpha_m$ are determined by application of Eq. (4). Shown in Figs. 4 and 8 are the results.

Intensity Prediction

As noted earlier, Sarpkaya's experiment indicated an oscillatory movement of several cycles prior to the final detachment of the first pair of vortices. This, according to our argument, would give rise to several small peaks in the nonzero side force plot. Unfortunately, since there are as yet no quantitative measurements or correlations, accurate prediction cannot be made at the present stage. There is, however, a reason to believe that the critical angle plotted in Fig. 9 corresponded to the first major local peak, and the smaller peaks prior to this were neglected in their measurement because the onset of flow asymmetry was estimated by the criterion that the lateral force exceeded 5% of the normal force. For this reason, nonzero side force prior to the critical angle is not considered.

The observations made in the published work and therefore the conclusions drawn were mainly for the purpose of understanding the phenomenon. It is not altogether satisfactory to apply them directly for calculation. Supplementary interpretation seems to be needed. To this end we introduce an idealization as follows: The initial formation from two symmetrical vortices to two asymmetrical ones takes place in the distance between g_1 and g_2. These two vortices at the point of g_2 viewed in the cross-flow plane are assumed to have the relative positions and strengths shown in Fig. 10a, in which the strengths of the vortices are dimensionless quantities in reference to the regular one. When the angle of attack is further increased, the next special state emerges in which g_2 moves forward and g_3 comes into contact with the body base. The formation of these two vortices reaches the second stage between g_2 and g_3 and comes to maturity at g_3. The relative position of the vortices is seen to be reversed and the intensity adjusted, with the vortex closer to the body growing stronger. Shown in Fig. 10b is the profile at g_3. If the incidence increases further, g_2 and g_3 will both move forward and decrease their absolute lengths simultaneously, leaving room for g_4 to contact the base lip. In the meantime, the third vortex begins its formation at g_3 and completes its process at g_4. This then is the first regular member of the vortex family with its intensity given by Eq. (3). This process of casting off more vortices in a given distance with alternate shedding of vorticity will continue as lonr as the incidence keeps increasing. The highest angle of attack before the change-over takes place is found to be $\alpha_5 = 46.5°$ for the F-5E fuselage model of which the vortex pattern is shown schematically in Fig. 10c.

At first sight, the value of vortex intensity in Fig. 10 are seen to be arbitrary. However, they are not chosen without any base. The careful measurement made by Thomson and Morrison and their schlieren pictures revealed that the first vortex is very weak and cannot be easily discerned or given a value of circulation. The second vortex is found to possess approximately one half the intensity of the regular vortex. The vortex model after g_3 is therefore established on the basis of this finding, with the first vortex obliterated altogether. Turning now to the vortex system prior to g_3, we reason that because the magnitude of the circulation C_4, C_5, . . . is only one half the intensity of each regular free vortex, the values in the formative stages must be smaller. To approximate this, two values $C_2 = C/4$ and $C_3 = 3C/4$ were thus selected with $C = |C_4|$ or $|C_5|$. It turned out that the estimated forces using these two values agree reasonably well with the test data. The intensity level for the circulations is thus fixed tentatively. The possibility of furture modification, of course, exists when further experimental data become available. The

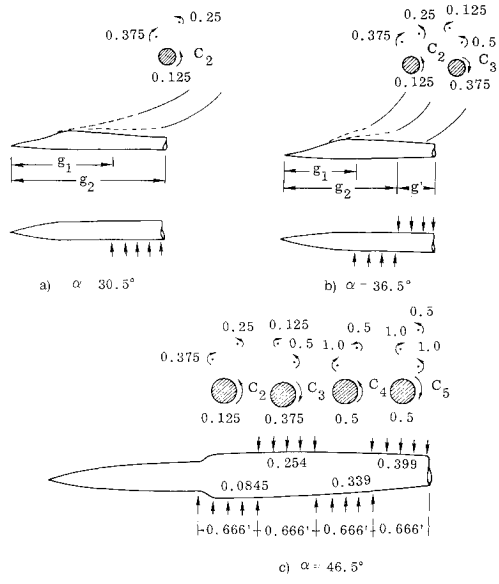

Fig. 10 Sketches of disposition of vortices in cross-flow planes.

strengths of field vortices are not really relevant to our prediction. However, for the sake of completeness, we still assign certain values to be found in Fig. 10.

The work which remains to be done before the actual computation is then to determine the strength of a regular free vortex by Eq. (3). For the fuselage model, Eq. (3) is used as it is but for the regular configuration such as the circular tangent ogive with afterbody the intensity obtained from Eq. (3) is reduced by a factor of 2/3, a ratio of the mean test data in Ref. 7 to the calculation. We have actually commented on this point earlier, but is repeated here for completeness.

Finally we shall introduce a further simplification that the circulation C_m be distributed uniformly in its interval from g_{m-1} to g_m. Application of Eq. (1) will then result in side force per unit length.

Since the computational procedure previously detailed is fairly involved and was not introduced in a sequential manner, it is perhaps worth recapitulating it. Following are the steps for making prediction of nonzero side force on a given body: a) Find the semiapex angle Θ_c, the fineness ratio f_r, and the mean diam d of the afterbody. b) Select the critical angle-of-attack α_c from the diagram for the onset of flow asymmetry (Fig. 9 or similar). c) Use Eq. (5) to determine B_c, the empirical constant. d) If the information for the onset of flow asymmetry was based on tests conducted at different Reynolds number range from the case under consideration, re-compute α_c as demonstrated in Eq. (6). e) Obtain angles-of-attack α_m for consecutive local peaks for $m \geq 3$ from Eq. (4). f) Determine the intensity Γ of a regular free vortex by Eq. (3). g) Select the circulation C_m for $m \geq 2$ in the interval g' between g_{m-1} and g_m in accordance with disposition of vortices shown in Fig. 10. h) Compute the lateral force per unit length from Eq. (1). i) Sum the lateral forces in intervals of g' to give the nonzero side force on the body.

Calculation and Remarks

The calculated nonzeros on a F-5E fuselage are indicated in Figs. 4 and 8 and compared with the test data in the same figures. The moment center for the yawing moment is 1.8 ft from the base of the 0.1 scale model; the symbol C_y and C_n in these figures are the lateral force and yawing moment coefficients given by force/$\frac{1}{2}\rho_\infty U_\infty^2 A$ and moment/$\frac{1}{2}\rho_\infty U_\infty^2 Ab$ respectively, with A (model wing area) = 1.86 ft^2 and b (model wing span) = 2.67 ft. The yawing moment is obtained by considering lateral force only. The "static" pressure due to

the big-scale flow[15] can affect the drag but will not have any contribution to the yawing moment for the moment center is located on the symmetric plane. The side force coefficient shown in Fig. 7 is based on the data plotted in Ref. 5 but is made dimensionless by referring to the present model wing area instead of the original reference base merely for the sake of consistency and facilitating comparison to the fuselage data.

The sense for the "first" peak at the critical angle of attack cannot be specified in advance and is in fact undetermined. However, once it is chosen, the remaining ones are fixed. This uncertainty also shows up in experiment in the manner that a slight change if alignment of the body axis will cause the entire vortex system to switch its sequence (see, for example, Ref. 8).

The prediction is seen to fail at $\alpha = 50°$ in Fig. 8. This is probably due to the flow change-over. The fact that nonzeros exhibit radically different characteristics at $\alpha \gtrsim 50°$ testifies this assertion.

Test Facilities, Model, and Instrumentation

Since our test data are at variance with those reported by Lamont and Hunt, it is worth stating some details. Particulars have actually been given by Franco together with drawings. However, since this report may not be readily available to some readers, a summary is presented here and much of it is in the form of quotations.

The test was conducted in Northrop 7 ft × 10 ft low-speed wind tunnel. This is a single return, closed throat wind tunnel with an operating static pressure of nominally atmospheric pressure and a mean temperature of 80°F. Reynolds number was approximately 1.6×10^6 per foot.

The model was a 10% scaled reproduction of the F-5E fuselage measured 4.5 ft long (Fig. 11) with such accessories as the nose boom, boundary layer gutter, antennas, etc included. Engine air inlet ducts were simulated and allowed free flowing internal air to exit at the model base. Boundary-layer transition strips were applied at the lips of inlet ducts. In addition to the fuselage, tests were also conducted with build-up configurations to a "complete" airplane model. Two examples are presented in Figs. 1 and 2. For the complete airplane model, all the control surfaces were at neutral positions.

The model was sting mounted on the Northrop-216 sting and two-parameter sting support with image strut. The aerodynamic loads were measured with the Northrop-18 six-component internal strain gage balance. The blockage was corrected using model projected cross-sectional area. The flow angularity in the test section was nominally zero. Some tests were done twice to check repeatability.

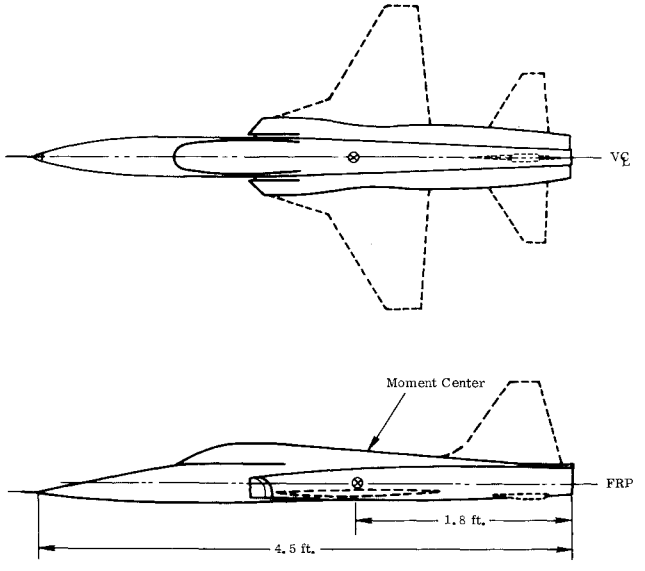

Fig. 11 10% scale F-5E fuselage and complete configuration models.

Conclusions

There is actually no lack of experimental work for an inclined body in a uniform flow, but for the most part the problem is only partially covered. Investigation is usually limited either to surveying the vortex formation and the field properties or to taking measurements for the forces and moments but not both. Although the present work is not experimental, it may still be regarded as an effort to bridge some of this gap and to thread a few isolated findings together.

Based on the extensive experiments by Thomson and Morrison[8] and others, a simple model has been proposed to describe low-speed flow characteristics of a slender body at high angles of attack and with zero sideslip angle. A prediction method resulting from this model with correlation parameters given by various investigators has been formulated to estimate nonzero side force and yawing moment on a F-5E fuselage model and an ogive-cylinder combination. The results obtained have been compared with test data and showed satisfactory agreement.

There undoubtedly remain many unsettled questions. For example, the inconsistency among test data from various sources should be dealt with effectually. If further experiments are to be conducted, some of the idealization and assumptions made here should perhaps also be checked.

The test conducted by Keener and Chapman[5] shows an abrupt rise in magnitude of nonzero side forces as R_D, the Reynolds number based on the reference diameter, increases from 0.8×10^6 to $2.0 \times 10.^6$ A further increase of the Reynolds number to 3.8×10^6 did not, however, show any significant change in side forces. In view of the fact that a similar thing also happens in the Strouhal number plot of Fig. 6, this is perhaps not altogether surprising. We presume that a change-over from laminar boundary layer to turbulent one will cause such a rise. The present method is applicable to low or moderately high Reynolds number cases as is evident from the comparisons made in Figs. 4, 7, and 8. This limitation seems to stem directly from the fact that the present method is in the large part based on the correlations found by Thomson and Morrison in their experiments of moderate Reynolds number, believing to possess laminar boundary layer only. These correlations would not be valid if the boundary layer is turbulent. It is equally evident by seeing the experimental result of Keener and Chapman for cases of $R_D = 2.0 \times 10^6$ and 3.8×10^6 that the present method is incapable of predicting such a high-level side force. We must, therefore, conclude that extension of this method to high Reynolds number cases is only possible provided that further correlations similar to the ones used here can be found. This may well be an important aspect to be considered in the future work, since the scaling effect must be accounted for in the application of any method to practical problems.

References

[1] Allen, H. J. and Perkins, E. W., "A Study of Effects of Viscosity on Flow Over Slender Inclined Bodies of Revolution," Rept. 1048, 1951, NACA.

[2] Letko, W., "A Low-Speed Experimental Study of the Directional Characteristics of a Sharp-Nosed Fuselage Through a Large Angle-of-Attack Range at Zero Angle of Sideslip," TN 2911, March 1953, NACA.

[3] Franco, B. G., "Data Report of a Low Speed High Attitude Wind Tunnel Test of a 0.1 Scale F-5E Force Model," NOR 72-31, March 1972, Northrop Corporation, Aircraft Division, Hawthorne, Calif.

[4] Coe, P. L., Chambers, J. R., and Letko, W., "Asymmetric Lateral-Directional Characteristics of Pointed Bodies of Revolution at High Angles of Attack," TN D-7095, Nov. 1972, NASA.

[5] Keener, E. R. and Chapman, G. T., "Onset of Aerodynamic Side Forces at Zero Sideslip in Symmetric Forebodies at High Angles of Attack," AIAA Paper 74-770, Anaheim, Calif., 1974.

[6] Lamont, P.J. and Hunt, B.L., "Out-of-Plane Force on a Circular

Cylinder at Large Angles of Inclination to a Uniform Stream," *Aeronautical Journal,* Vol. 77, No. 745, Jan. 1973, pp. 41-45.

[7] Wardlaw, A.B., "Prediction of Yawing Force at High Angle of Attack," *AIAA Journal,* Vol. 12, No. 8, Aug. 1974, pp. 1142-1144.

[8] Thomson, I.D. and Morrison, D.F., "The Spacing, Position and Strength of Vortices in the Wake of Slender Cylindrical Bodies at Large Incidence," *Journal of Fluid Mechanics,* Vol. 50, Pt. 4, Dec. 1971, pp. 751-783.

[9] Sarpkaya, T., "Separated Flow About Lifting Bodies and Impulsive Flow About Cylinders," *AIAA Journal,* Vol. 4, March 1966, pp. 414-420.

[10] Prandtl, L. and Tietjens, O. G., *Applied Hydro – And Aeromechanics,* Dover, New York, 1957.

[11] Milne—Thomson, L. M., *Theoretical Hydrodynamics,* 5th ed., Macmillan, New York, Chapt. 8, 13, 16.

[12] Sarpkaya, T., "Lift, Drag, and Added Mass Coefficients for a Circular Cylinder Immersed in a Time-Dependent Flow," *ASME Transactions; Journal of Applied Mechanics,* Vol. 30, Ser. E, No. 1, March 1963, pp. 13-15.

[13] Peake, D.J., Rainbird, W.J., and Atraghji, E.G., "Three-Dimensional Flow Separations on Aircraft and Missiles," *AIAA Journal,* Vol. 10, May 1972, pp. 567-580.

[14] Morkovin, M. V., "Flow Around Circular Cylinder—A Kaleidoscope of Challenging Fluid Phenomena," *Symposium on Fully Separated Flows,* edited by A. G. Hansen, American Society of Mechanical Engineers, May 1964.

[15] Lighthill, M.J., "Mathematics and Aeronautics," *Journal of the Royal Aeronautical Society,* Vol. 64, No. 595, July 1960, pp. 375-393.